

Prolonged viral shedding from noninfectious individuals confounds wastewater-based epidemiology

Tin Phan¹, Samantha Brozak², Bruce Pell³, Stanca M. Ciupe⁴, Ruian Ke¹, Ruy M. Ribeiro¹, Anna Gitter^{5,6}, Kristina D. Mena^{5,6}, Alan S. Perelson^{1,7}, Yang Kuang², and
Fuqing Wu^{5,6*}

¹ Theoretical Biology and Biophysics, Los Alamos National Laboratory, NM 87544, USA.

² School of Mathematical and Statistical Sciences, Arizona State University, AZ 85281, USA.

³ Department of Mathematics and Computer Science, Lawrence Technological University, MI 48075, USA.

⁴ Department of Mathematics, Virginia Tech, Blacksburg, VA 24060, USA.

⁵ School of Public Health, The University of Texas Health Science Center at Houston, Houston, TX 77030, USA.

⁶ Texas Epidemic Public Health Institute, TX, USA.

⁷ Santa Fe Institute, Santa Fe, NM 87501, USA.

* Corresponding author: Fuqing Wu

Email: Fuqing.Wu@uth.tmc.edu

Keywords: wastewater-based epidemiology, prolonged viral shedding, mathematical modeling, transmission dynamics.

1 **Abstract**

2 Wastewater surveillance has been widely used to track and estimate SARS-CoV-2
3 incidence. While both infectious and recovered individuals shed virus into wastewater,
4 epidemiological inferences using wastewater often only consider the viral contribution
5 from the former group. Yet, the persistent shedding in the latter group could confound
6 wastewater-based epidemiological inference, especially during the late stage of an
7 outbreak when the recovered population outnumbered the infectious population. To
8 determine the impact of recovered individuals' viral shedding on the utility of wastewater
9 surveillance, we develop a quantitative framework that incorporates population-level viral
10 shedding dynamics, measured viral RNA in wastewater, and an epidemic dynamic
11 model. We find that the viral shedding from the recovered population can become higher
12 than the infectious population after the transmission peak, which leads to a decrease in
13 the correlation between wastewater viral RNA and case report data. Furthermore, the
14 inclusion of recovered individuals' viral shedding into the model predicts earlier
15 transmission dynamics and slower decreasing trends in wastewater viral RNA. The
16 prolonged viral shedding also induces a potential delay in the detection of new variants
17 due to the time needed to generate enough new cases for a significant viral signal in an
18 environment dominated by virus shed by the recovered population. This effect is most
19 prominent toward the end of an outbreak and is greatly affected by both the recovered
20 individuals' shedding rate and shedding duration. Our results suggest that the inclusion
21 of viral shedding from non-infectious recovered individuals into wastewater surveillance
22 research is important for precision epidemiology.

23 **Introduction**

24 SARS-CoV-2 concentration in wastewater is strongly correlated to case report data ($R >$
25 0.7) (1), supporting the effort of using wastewater-based epidemiology (WBE) to
26 estimate infection incidence (2, 3). However, gastrointestinal tract viral shedding exhibits
27 great heterogeneity among individuals, and a significant portion of clinically recovered
28 individuals (i.e., individuals who are no longer infectious) shed virus in fecal specimens
29 for weeks to months after the infectious phase (4-7). As an outbreak progresses, the
30 number of recovered individuals accumulates, which results in an increase in their
31 contribution to the overall viral RNA load in wastewater. While the prolonged shedding of
32 SARS-CoV-2 in feces is well documented (4-6), to what extent the persistent shedding
33 impacts the epidemiological inference of wastewater data remains unexplored.

34 Based on recent studies, we propose the integration of wastewater data with within-host
35 (viral shedding dynamics) and between-host (transmission dynamics) models to
36 demultiplex the viral shedding from infectious and recovered phases (8, 9). The central
37 idea is to use a population-level viral shedding profile, segmented according to the
38 infection state, to connect viral RNA in wastewater with standard transmission dynamics
39 models (SI Appendix). Our goal is to examine the potential impact of the virus shed by
40 the recovered population on the capability of WBE to capture the epidemic landscape.

41

42 **Results and Discussion**

43 **Viral shedding by the recovered population alters the correlation of virus**

44 **measured in wastewater and case report data.** We fit a Susceptible-Exposed-
45 Infectious-Recovered-Virus (SEIR-V) model (Eq. 1, SI Appendix) including a population
46 viral shedding function (Eq. 5, SI Appendix) to viral RNA measurements in wastewater
47 collected from the Greater Boston area from 10/01/2020 to 02/27/2021 (1, 3), under the

48 assumption that individuals who stop shedding virus are removed from the recovered
49 class. The time frame was chosen to limit the data to a single wave of the COVID-19
50 pandemic (Alpha variant B.1.1.7) when the vaccination rate was low in the population.
51 For a proof-of principle demonstration, we assume that recovered individuals on average
52 shed virus at 50% of the mean viral shedding rate of infectious individuals for 14 days.
53 The model captures the viral dynamics in wastewater well and the inferred transmission
54 dynamics reflect the trend of the reported incidence (Fig. 1A-B). The model-predicted
55 transmission dynamics, however, precede the reported incidence by about 3 weeks (as
56 compared by peak timing – vertical dashed lines in Fig. 1B). The model-inferred
57 incidence exceeds the reported daily incidence by 3-5 times near the beginning of Oct.
58 and at the end of Feb. and over 10 times around Dec. Both observations are consistent
59 with the expected lead time of wastewater data relative to case report data and the
60 underreported incidence rates (10, 11).

61
62 Next, we compared the dynamics of the infectious and the recovered populations. As
63 shown in Fig. 1C, the number of recovered individuals increases quickly and exceeds
64 the infectious population. While the infectious population contributes most of the viral
65 RNA in wastewater near the beginning of this epidemic wave, the recovered population
66 eventually surpassed their viral contribution. Although these quantitative results may
67 vary with different assumed viral shedding rates and shedding durations for the
68 recovered population, they show how the viral shedding from the recovered population
69 becomes more significant as an outbreak progresses.

70
71 The increase of virus shed by the recovered population creates a transient period where
72 wastewater data may not directly reflect the incidence and dynamics of active infection.

73 An intuitive approach to validate this inference is by comparing the correlation between
74 wastewater viral measurements and reported incidence using data spanning different
75 phases of an outbreak. During the early phase of an outbreak, wastewater data should
76 be highly correlated with the reported daily new cases since the infectious population
77 contributes substantially more virus to wastewater. However, the correlation should
78 decrease as the outbreak progresses with the increase of the virus shed by the
79 recovered population. We explicitly demonstrated this point by fitting the same model to
80 increasingly larger data sets (Fig. 1D and 1E). We observe a clear decreasing trend in
81 the correlation coefficient between the model-inferred daily incidence and the reported
82 daily incidence with the inclusion of data post-transmission peak. Additionally, the
83 model-simulated correlations (SI Appendix) between daily viral measurement and
84 incidence show that the inclusion of viral shedding by the recovered population predicts
85 a faster decline of the correlation coefficient as the outbreak progresses (Fig. 1F). Note
86 that the increasing trend near the end is a result of the convergence of daily viral
87 measurement in wastewater and incidence at the end of the outbreak. Thus, the
88 exclusion of the virus shed by the recovered population is likely to have a small effect on
89 the model-inferred transmission dynamics in the early phase of an outbreak (Fig. 1D and
90 1F). However, when using wastewater surveillance to track emerging cases toward the
91 end of an outbreak or to connect multiple waves, it is necessary to include the virus shed
92 by the recovered population to accurately capture transmission.

93

94 **Inclusion of recovered shedding predicts an earlier peak time of the outbreak.** To
95 better explain the mechanisms behind the changes in the correlation between
96 wastewater data and case report data, we tested the impact of varied shedding rates
97 and duration from the recovered individuals on model-inferred transmission dynamics.

98 Fig. 2A shows the model fitting to viral load in wastewater under three scenarios: 1) no
99 shedding from recovered individuals, 2) HRMD: high recovered shedding rate (75% of
100 the infectious shedding rate) for a moderate duration of 14 days, 3) MRLD: moderate
101 recovered shedding rate (50% of the infectious shedding rate) with a long duration of 21
102 days. Model fits under the three scenarios are similar, but the higher shedding rates and
103 longer shedding durations result in slightly slower decreasing trends of the total viral load
104 (Fig. 2A). A remarkable difference is observed in the daily incidence. The inclusion of
105 viral shedding by the recovered population shifts the transmission peak by 6- and 10-day
106 earlier under MRLD and HRMD scenarios, respectively (vertical dashed lines, Fig. 2B).
107 These results suggest that the actual incidence peak time of the Alpha variant outbreak
108 may be much earlier than the clinically reported cases and the change in the correlation
109 is due in part to the differences in the viral shedding dynamics between the infectious
110 and the recovered phases.

111

112 **The virus shed by the recovered population leads to a delay in the detection of an**
113 **emerging variant by WBE.** Several studies have looked at the minimum number of new
114 cases required for the detection of virus in wastewater (12-14); however, none has
115 looked into this issue in the presence of uncertainty due to the viral shedding from the
116 recovered population. This is especially important during a transition period when a new
117 variant is emerging near the end of an ongoing outbreak (Fig. 2C). The viral shedding
118 from a large number of recovered individuals in wastewater may overshadow the viral
119 shedding from new cases infected with the new variant, therefore undermining a rapid
120 recognition of the emergence of the new variant based on the viral load in wastewater.
121 We used the SEIR-V model to further quantify the relationship between shedding from
122 recovered population and shedding from individuals with the new variant. Assuming the

123 emerging variant has a similar viral shedding rate to its predecessor, we found that the
124 number of required infectious cases with the new variant to signal an emerging outbreak
125 is an increasing function of both the viral shedding rate and shedding duration of the
126 recovered population (Fig. 2D, warmer colors). Since it takes time to generate the
127 required number of infections for detection, this implies an increasing delay in the
128 detection of an emerging outbreak as more new infections are needed. This delay is
129 minimized if the viral shedding rate of the new variant is significantly higher than its
130 predecessor (data not shown). Thus, tracking the viral shedding from the recovered
131 population is important to mitigate the delay in the detection of new variants based on
132 wastewater data.

133

134 The identification and mitigation of this time delay requires an accurate description of the
135 population viral shedding profile, which may be variant-specific. Thus, integrating
136 modeling analysis of routine wastewater surveillance data and genomic sequencing of
137 wastewater samples (15) may better facilitate the identification of emerging variants
138 circulating in the community. While our analysis focuses on the end of an outbreak to
139 highlight the impact of prolonged shedding, similar analyses can be carried out to study
140 the detection delay at different times during the outbreak and may need to account for
141 the viral shedding from both the infectious and recovered population if they are not
142 negligible.

143

144 In summary, we show that an understanding of the relative viral shedding during each
145 phase of an infection is crucial to the implementation of precision WBE, which transpires
146 beyond the study of the correlation between viral measurement in wastewater and case
147 report data. Prolonged shedding can alter model-inferred transmission dynamics and

148 lead to a delay in detection if not accounted for. Our analyses provide a proof-of-
149 principle framework to quantify the impact of prolonged fecal shedding on wastewater-
150 based estimation of new infections and the outbreak progression.

151

152 **Materials and Methods**

153 See SI Appendix.

154

155 **Data and Code Availability**

156 The authors declare that the data and code will be provided with the publication of this
157 study.

158

159 **Author Contributions**

160 T.P., R.K., R.M.R., Y.K., and F.W. designed research; T.P., S.M., B.P., and F.W.
161 performed research; T.P., S.M., R.K., R.M.R., K.D.M., A.S.P., Y.K., F.W. contributed
162 new reagents/analytic tools; T.P., S.M., B.P., S.M.C., R.K., R.M.R., A.G., and F.W.
163 analyzed data; and T.P., S.M., B.P., S.M.C., R.K., R.M.R., A.G., K.D.M., A.S.P., Y.K.,
164 and F.W. wrote the paper.

165

166 **Acknowledgments**

167 This work is supported by Faculty Startup funding from the Center of Infectious Diseases
168 at UTHealth, the UT system Rising STARS award, and the Texas Epidemic Public Health
169 Institute (TEPHI) to F.W. This work was also supported by the Director's postdoctoral
170 fellowship at Los Alamos National Laboratory to T.P.; Y.K. and S.B. are partially supported
171 by the US National Science Foundation Rules of Life program DEB -1930728 and the NIH
172 grant 5R01GM131405-02.

173

174 **Competing Interest Statement**

175 The authors declare no competing interest.

176

177 **References**

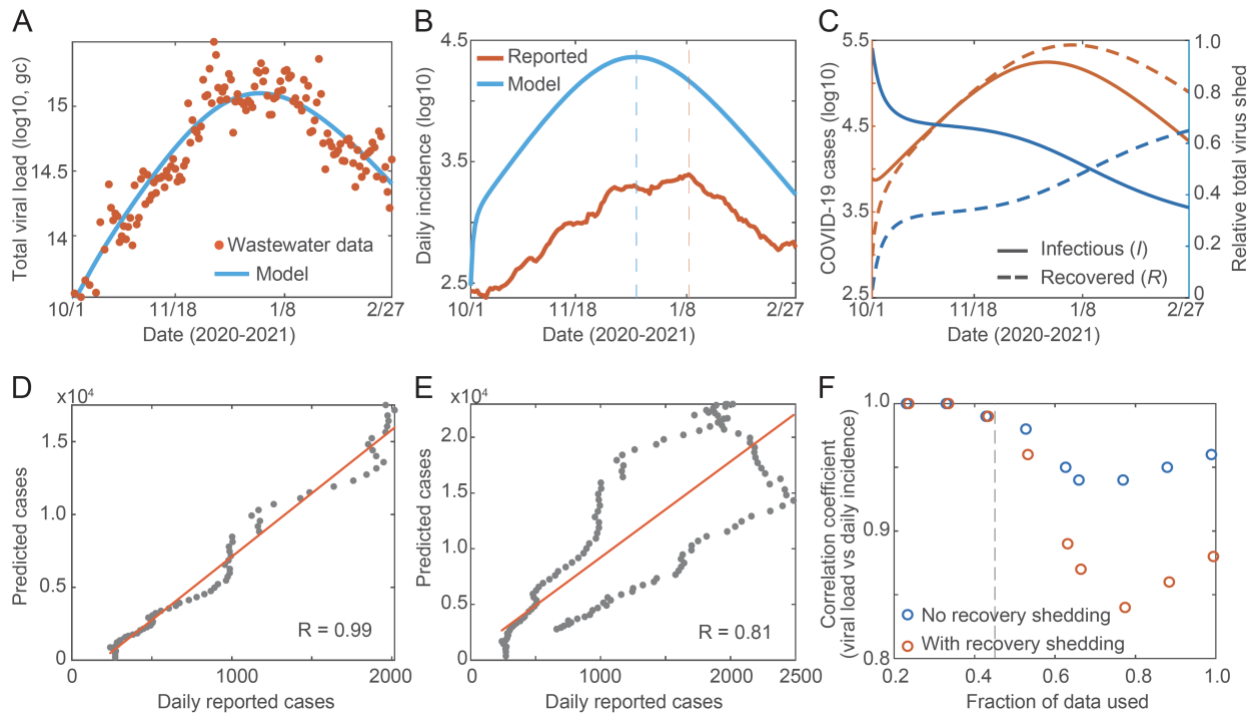
- 178 1. F. Wu, et al., SARS-CoV-2 RNA concentrations in wastewater foreshadow
179 dynamics and clinical presentation of new COVID-19 cases. *Sci. Total Environ.*
180 805, 150121 (2022).
- 181 2. P. Kilaru, et al., Wastewater surveillance for infectious disease: a systematic
182 review. *Am. J. Epidemiol.* 192(2), 305-322 (2023).
- 183 3. A. Xiao, et al., Metrics to relate COVID-19 wastewater data to clinical testing
184 dynamics. *Water Res.* 212, 118070 (2022).
- 185 4. S. Gupta, J. Parker, S. Smits, J. Underwood, S. Dolwani, Persistent viral
186 shedding of SARS-CoV-2 in faeces—a rapid review. *Colorectal Dis.* 22(6), 611-
187 20 (2020).
- 188 5. M. Cevik, et al., SARS-CoV-2, SARS-CoV, and MERS-CoV viral load dynamics,
189 duration of viral shedding, and infectiousness: a systematic review and meta-
190 analysis. *The Lancet Microbe.* 2(1), e13-22 (2021).
- 191 6. A. Natarajan, et al., Gastrointestinal symptoms and fecal shedding of SARS-
192 CoV-2 RNA suggest prolonged gastrointestinal infection. *Med* 3(6), 371-387
193 (2022).
- 194 7. B. Killingley, et al., Safety, tolerability and viral kinetics during SARS-CoV-2
195 human challenge in young adults. *Nature Med.* 28(5), 1031-1041 (2022).

- 196 8. T. Phan, et al., A simple SEIR-V model to estimate COVID-19 prevalence and
197 predict SARS-CoV-2 transmission using wastewater-based surveillance data.
198 *Sci. Total Environ.* 857, 159326 (2023).
- 199 9. B. Pell, S. Brozak, T. Phan, F. Wu, Y. Kuang, The emergence of a virus variant:
200 dynamics of a competition model with cross-immunity time-delay validated by
201 wastewater surveillance data for COVID-19. *J. Math. Biol.* 86(5), 1-34 (2023).
- 202 10. F. Wu, et al., SARS-CoV-2 titers in wastewater are higher than expected from
203 clinically confirmed cases. *mSystems* 5(4), e00614-20 (2020).
- 204 11. F. J. Angulo, L. Finelli, D. L. Swerdlow, Estimation of US SARS-CoV-2
205 infections, symptomatic infections, hospitalizations, and deaths using
206 seroprevalence surveys. *JAMA Netw. Open* 4(1), e2033706-e2033706 (2021).
- 207 12. J. Hewitt, et al., Sensitivity of wastewater-based epidemiology for detection of
208 SARS-CoV-2 RNA in a low prevalence setting. *Water Res.* 211, 118032 (2022).
- 209 13. P. Y. Hong, et al., Estimating the minimum number of SARS-CoV-2 infected
210 cases needed to detect viral RNA in wastewater: To what extent of the outbreak
211 can surveillance of wastewater tell us? *Environ. Res.* 195, 110748 (2021).
- 212 14. M. Nauta, et al., Early detection of local SARS-CoV-2 outbreaks by wastewater
213 surveillance: a feasibility study. *Epidemiol. Infect.* 151, e28 (2023).
- 214 15. S. Karthikeyan, et al., Wastewater sequencing reveals early cryptic SARS-CoV-
215 2 variant transmission. *Nature* 609, 101-108 (2022).

216
217
218
219
220

221 **Figures**

222



223

224

225 **Figure 1. Viral shedding from the recovered population alters the correlation of**

226 **virus measured in wastewater and case report data.** Predicted viral dynamics

227 obtained from fitting model Eq. 1 to viral shedding data of both infectious and recovered

228 individuals. **(A)** Theoretical viral dynamics (blue curve) obtained by fitting the daily

229 production of V in Eq. 1 to daily measurements of viral RNA (brown dots) in wastewater

230 for the Greater Boston area. **(B)** Model-predicted daily incidence (blue line) vs. reported

231 incidence (brown curve). The vertical dashed lines are the incidence peak time. **(C)** Left

232 y-axis: model predicted number of infectious (solid brown curve) and recovered

233 individuals (dotted brown curve). Right y-axis: relative contribution to the viral RNA

234 measurements from the infectious (solid blue curve) and recovered (dotted blue curve)

235 populations. **(D-E)** The correlation coefficient between predicted cases and reported

236 cases decreases as more data are used for the fitting (within one wave). D only uses
237 pre-peak data. E contains increasingly more data after the peak. (F) The model-
238 predicted correlation between daily viral measurements in wastewater and daily
239 incidence with and without the recovered shedding in the model. If the fraction of data
240 used is 1, the data for one entire outbreak is used for the correlation. The vertical
241 dashed line indicates the transmission peak.

242

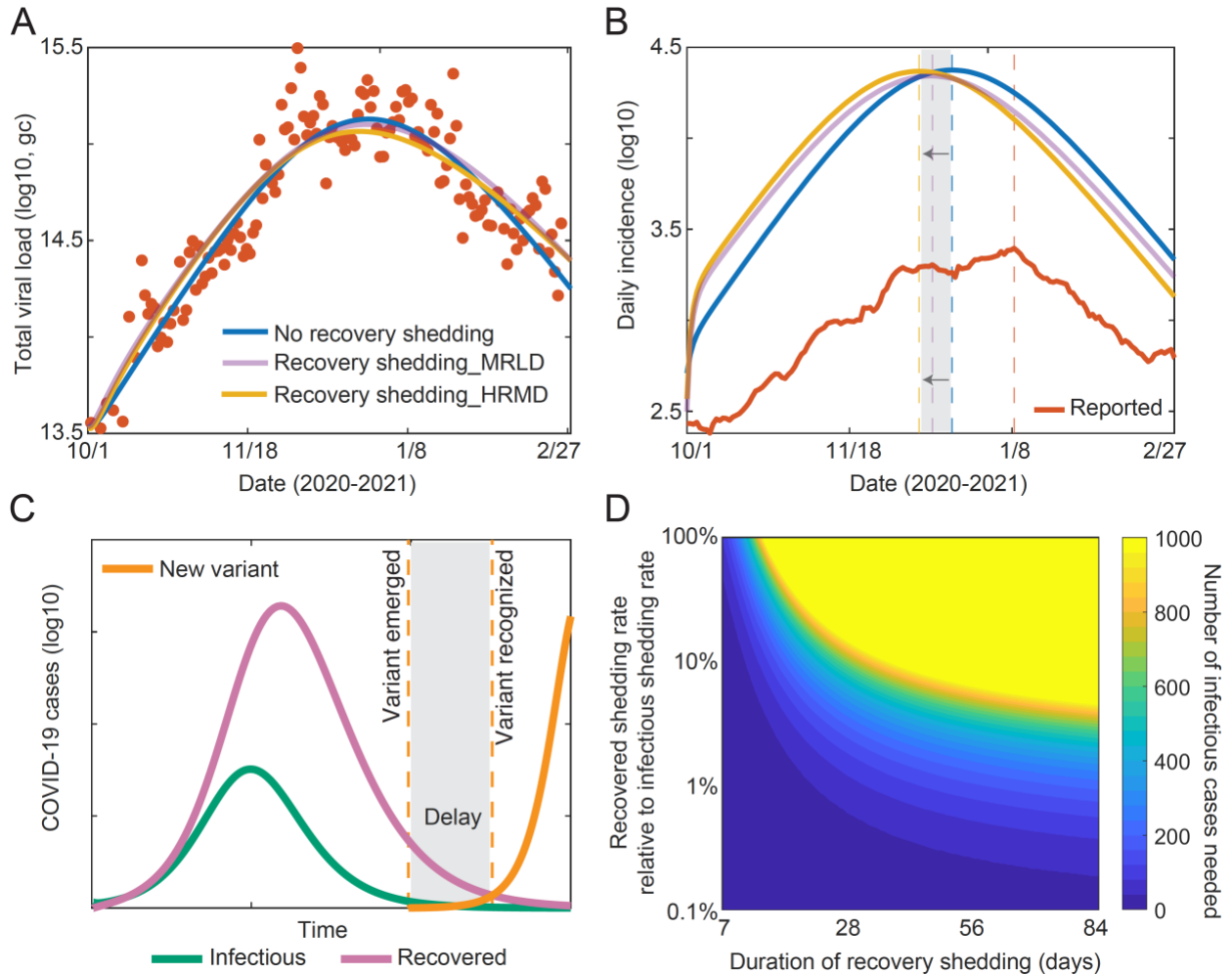
243

244

245

246

247



248

249

250 **Figure 2. The inclusion of recovered shedding predicts an earlier peak time of the**
 251 **outbreak and a delay in the detection of an emerging variant by WBE. (A)** Viral RNA
 252 in wastewater under different recovered shedding scenarios. Each model was fit to data
 253 from 10-01-2020 to 02-27-2021, which was chosen to restrict the outbreak to a single
 254 variant (brown data points). **(B)** Model inferred daily incidence under three recovered
 255 shedding scenarios. The vertical dashed curves are the corresponding peak times. **(C)** A
 256 schematic of tracking the emergence of a new variant near the end of an outbreak when
 257 most of the virus measured comes from the recovered population. **(D)** The number of
 258 new infectious cases needed to produce a sufficiently large viral signal, which depends

259 on the recovered shedding rate and duration (Eqs. 9-11, SI Appendix). Warmer colors
260 refer to a higher number of cases. This snapshot was taken when the outbreak reached
261 99.9% of its final size (as depicted by **C**) to show the potential of WBE to capture an
262 emerging outbreak.

1
2
3
4
5
6
7
8
9
10
11
12
13
14
15
16
17
18

Supplementary Materials

Prolonged viral shedding from noninfectious individuals confounds wastewater-based epidemiology

Tin Phan¹, Samantha Brozak², Bruce Pell³, Stanca M. Ciupe⁴, Ruian Ke¹, Ruy M. Ribeiro¹, Anna Gitter⁵, Kristina D. Mena^{5,6}, Alan S. Perelson^{1,7}, Yang Kuang², and Fuqing Wu^{5,6,*}.

*Corresponding author: Fuqing Wu

Email: Fuqing.Wu@uth.tmc.edu

This PDF file includes:

Supporting text

SI References

19 **Methods**

20

21 **S1. SEIR-V model with temperature variation.**

22

23 We modified the SEIR-V model in Phan et al. (1) to include viral shedding from both the infectious
24 and recovered populations. We also initially examined the viral shedding from the exposed class,
25 which turned out to be negligible, due to the low shedding rate and short duration of the exposed
26 class (not shown). Its implications are discussed in S6.

27

28 *Equation 1*

29

$$S' = -\lambda IS$$

30

$$E' = \lambda IS - kE$$

31

$$I' = kE - \delta I$$

32

$$R' = (1 - \epsilon)\delta I - \sigma R$$

33

$$V' = \alpha(1 - \gamma(T))(\beta_I I + \beta_R R).$$

34

35 S is the susceptible population, E is the exposed population, I is the infectious population, and R
36 is the recovered population that still sheds virus. Susceptible individuals are infected at a rate λI .
37 Exposed individuals take on average $1/k$ days before becoming infectious. Infectious individuals
38 recover or die after an average duration of $1/\delta$ days. The disease-induced mortality rate is ϵ .
39 However, since SARS-CoV-2-induced mortality is small, we set $\epsilon = 0$ for simplicity. Recovered
40 individuals shed virus for an average duration of $1/\sigma$ days. The cumulative viral RNA in
41 wastewater (V) is contributed by both infectious and recovered individuals in this model at rates
42 β_I and β_R , respectively, as opposed to the model proposed by Phan et al. (1). α is the average
43 fecal load per day. $\gamma(T)$ is the fraction of virus lost in wastewater between shedding and collection
44 (for measurement), which is assumed to be temperature-dependent (T). The temperature
45 variation over the duration of the study is fitted to average daily temperature data (1) in Celsius.

46

47 Equation 2

$$48 \quad T(t) = 3.6249 \sin(0.0202t - 4.4665) + 16.2298.$$

49

50 Where t is measured in days and $t = 0$ is 10/01/2020, see Fig. S1 in (1). The temperature-
51 adjusted half-life is assumed to be an exponential decay of the form:

52

53 Equation 3

$$54 \quad \eta(T) = \eta_0 Q_{10}^{-(T(t)-T_0)/10},$$

55

56 with η_0 being the half-life (hours) at ambient temperature T_0 and Q_{10} ($= 2.5$) being the
57 temperature-dependent rate of change (1, 2). The temperature-dependent decay rate $\xi(T)$ is
58 approximated by a first-order decay function, which gives: $\xi(T) = \frac{\ln 2}{\eta(T)}$. Assume viral RNA decays
59 exponentially ($V' = -\xi(T)V$ or $V(t) = V_0 e^{-\xi(T)t}$), then the fraction of virus decay between
60 shedding and collection is given by:

61

62 Equation 4

$$63 \quad \gamma(T) = \frac{V_0 - V(t_{arrive})}{V_0} = 1 - e^{-\xi(T)t_{arrive}}.$$

64

65 Here, t_{arrive} is the time between shedding and collection, which we take to be 24 hours. The loss
66 fraction γ is approximated between 0.03-0.28 for varying travel times and temperature, see SI in
67 (1). However, this loss fraction could also be a function of the biochemical composition of the
68 wastewater and microorganism community in the sewer. For example, an extremely harsh
69 environment may result in a shorter viral half-life, which implies that the sample may be mostly
70 influenced by viruses shed closer to the time of sampling.

71

72 Finally, we remark that $V(t)$ is a proxy variable for the cumulative virus shed in wastewater. Its

73 daily difference ΔV_t , which represents the virus measured on day t is the quantity of interest, e.g.,

74 $\Delta V_t = V(t) - V(t - 1)$. Similarly, we estimate the daily incidence by looking at the cumulative
75 number of infectious individuals. This is done by creating another proxy variable $C(t)$ with $C'(t) =$
76 kE and taking the daily difference ΔC_t to be the daily incidence on day t , e.g., $\Delta C_t = C(t) -$
77 $C(t - 1)$. Note that while ΔC_t is a good approximation, it does not perfectly correspond to the daily
78 report data, which varies based on many factors such as report time and symptom onset.

79

80 ***S2. The population level viral shedding function.***

81

82 The viral dynamics within an infected individual is relatively well defined (3, 4) and can be
83 described by standard models of viral dynamics (5). Here, to simplify, we describe the viral levels
84 in the gastrointestinal tract, which is proportional to the viral shedding rate, using a
85 phenomenological function introduced by Phan et al. (1):

86

87 *Equation 5*

88

$$f(t) = \frac{\omega_1 t}{\omega_2^2 + t^2},$$

89

90 which peaks at $\frac{\omega_1}{2\omega_2}$ when $t = \omega_2$. Here, ω_1 (log10 viral RNA copy per g) is a magnitude modifier
91 and ω_2 (day) influences the timing and magnitude of the viral shedding peak. Note that the viral
92 shedding rate represents the viral concentration (per g of fecal matter) per day. This function has
93 been shown to be a good approximation for the viral shedding dynamics (1). With this function,
94 the total shedding between times t_1 and t_2 is given by

95

96 *Equation 6*

97

98

$$\int_{t_1}^{t_2} f(t) dt = \frac{\omega_1}{2} \log \left(\frac{\omega_2^2 + t_2^2}{\omega_2^2 + t_1^2} \right)$$

99

100 Where $0 \leq t_1 < t_2$ and \log denotes the natural logarithm. We remark that the unit of $f(t)$ is log10
101 viral RNA copy per g per day, meaning the integral $\int f(t)dt$ has unit of log10 viral RNA copy per
102 g.

103

104 The average exposed E , infectious I , and recovered with shedding R phases of an infection are
105 classified based on the time since infection (S_1). Thus, we can define t_E, t_I , and t_R (or $1/k, 1/\delta$,
106 and $1/\sigma$) to be the average time an infected person spent in these infection phases, respectively.

107 The average viral shedding rate during the infectious phase β_I can be determined by calculating
108 the average viral shedding over the infectious duration:

109

110 *Equation 7*

111

$$112 \quad \beta_I = \frac{1}{t_I} \int_{t_E}^{t_E+t_I} f(t) dt = \frac{1}{t_I} \frac{\omega_1}{2} \log \left(\frac{\omega_2^2 + (t_E + t_I)^2}{\omega_2^2 + t_E^2} \right)$$

113

114 Note that the unit of β_I is log10 viral RNA copy per g per day. Based on the best-fit to the viral
115 shedding data (1), we take $\omega_1 = 71.97$ log10 viral RNA copy per g and $\omega_2 = 4$ days. The
116 estimated value of β_I with $t_E = 3$ days and $t_I = 8$ days is 7.65 log10 viral RNA copy per g per
117 day. The viral shedding rate for the recovered population β_R is assumed to be a fraction of β_I . For
118 instance, the example in Fig. 1 assumes $\beta_R = 0.5 \times \beta_I$ and $t_R = 14$ days.

119

120 **S3. Data fitting.**

121

122 When fitting the SEIR-V model to the viral RNA data in wastewater, we minimize the difference
123 (SSE) between the measurement collected every 24-hour and the total virus produced at each
124 time data point. Here, $\hat{V}(t_d)$ is the total virus (e.g., viral RNA concentration \times total flow) measured
125 on day t_d , where t_d is the time of the measurement. $V(t)$, as given by Eq. 1, is a proxy of the

126 cumulative viral RNA in wastewater. Thus, the viral RNA produced daily, given by $\int_{t_{d-1}}^{t_d} V'(s)ds$,
127 or ΔV_t , is the comparable quantity to the viral RNA measured every 24-hour.

128

129 *Equation 8*

130
$$SSE = \sum_{t_d} \left(\log \int_{t_{d-1}}^{t_d} V'(s)ds - \log \hat{V}(t_d) \right)^2.$$

131

132 The computational minimization procedure is done using the function *fmincon* and *multistart*
133 (500 random initial guesses) in MATLAB.

134

135 The best-fit in Fig. 1A gives $\lambda = 9.36 \times 10^{-8}$ per day per person, $\alpha = 126$ g, and $E(0) = 145$
136 people. Note that the initial for the infected population is approximated by $I(0) = \frac{V(0)}{\alpha\beta(1-\gamma)}$, where
137 $V(0)$ is taken as the first viral RNA measurement and $E(0)$ and $R(0)$ are assumed to be 0. The
138 parameters k and δ are fixed to 1/3 and 1/8 per day, respectively (3), and σ is fixed to 1/14 per
139 day for the scenario in Fig. 1.

140

141 ***S4. Theoretical correlation between daily viral measurement and incidence with and***
142 ***without recovered shedding.***

143 We use the model to demonstrate how recovered shedding may affect the correlation between
144 viral measurements and incidence. The methods that are often used to relate daily viral
145 measurements to incidence data vary in literature (6, 7). However, here, we will simply look at the
146 correlation of daily viral measurement (ΔV_t) and incidence (ΔC_t). To produce Fig. 1I, we use the
147 best fit parameters for Fig. 1A (given in S3). The model without recovered shedding has $\beta_R = 0$.

148

149 ***S5. Simulation study of the impact of recovered shedding on the capability of WBE.***

150

151 One aspect of our study is to understand how the population average viral shedding profile
152 affects the sensitivity of wastewater surveillance data to track new cases over the course of an
153 outbreak. Since the viral shedding function $f(t)$ is fixed in structure and was fitted to only one
154 data set, it may not be able to fully capture the true dynamics of viral shedding. Thus, we want to
155 examine how variations in β_R and σ (or $1/t_R$) affect the model inferred transmission dynamics. To
156 focus our analysis on the impact of viral shedding from the recovered individuals, we vary only
157 the recovered shedding rate β_R and the duration σ while keeping all other parameters in the
158 model (Eq. 1) fixed as follow: $k = 1/3$ per day, $\delta = 1/8$ per day, $\lambda = 4 \times 10^{-7}$ per person per day,
159 $\alpha = 125$ g, $\gamma = 0.1$, $\beta_I = 7.65$ log₁₀ viral RNA copy per g per day, $S(0) = 1 \times 10^6$ people, $E(0) = 1$
160 person, $I(0) = 1$ person, and $R(0) = 1$ person.

161
162 The net virus shed by the R class varies over the course of an outbreak. Here, we limit the
163 analysis to the end of an outbreak, where virus shed by the recovered population contributes
164 close to 100% of viral measurements. In this scenario, to detect a significant change in the virus
165 in wastewater, we need enough new infections (or infectious cases) that can generate at least 5%
166 (assumed) of the viral shed by the recovered population on day t_d denoted by

167

168

169 *Equation 9*

170
$$C_R(t_d) = \int_{t_d-1}^{t_d} \alpha(1-\gamma)\beta_R R(t) dt.$$

171

172 Let $N(t_d)$ be the minimum number of new infections needed to match the viral signal from the
173 recovered population, then $N(t_d)$ must satisfy:

174

175 *Equation 10*

176
$$N(t_d)\alpha(1-\gamma)\beta_I > 0.05 C_R(t_d).$$

177

178 Solving for N , we have

179

180 *Equation 11*

181
$$N(t_d) > \frac{0.05 C_R(t_d)}{\alpha(1-\gamma)\beta_I}.$$

182

183 For reporting purposes (Fig. 2C-D), we round up N to the nearest integer. The heat map (Fig. 2D)

184 is generated by calculating N for the average recovered shedding rate β_R varying between 0.001

185 to 1 of β_I and the average recovered shedding duration σ varying between 1/7 to 1/84 per day

186 (or an average recovered shedding duration from 1 week to 12 weeks). The relative time (99.9%)

187 of the outbreak is defined as the time when the cumulative recovered population given by

188 $\int_0^t \delta I(s) ds$ reaches 99.9% of its final size $\left(\lim_{t \rightarrow \infty} \int_0^t \delta I(s) ds\right)$.

189

190 **S6. Further considerations.**

191

192 Our analyses ignore an intrinsic detection delay with WBE due to the low viral shedding of the

193 exposed phase. Exposed individuals likely shed virus at a very low rate compared to infectious

194 and recovered individuals. Thus, it is logical to assume that WBE is unlikely to detect the virus

195 shed by an exposed individual during an ongoing outbreak, leading to an intrinsic detection delay

196 of new cases using WBE. This detection delay may not be longer than 5 days, which is the

197 average time from infection to symptom onset, signaling high respiratory tract viral load (3). This

198 issue could be studied in detail if an accurate population level viral shedding dynamics is

199 available. However, to our knowledge, there has not been reported data on virus shed from the

200 gastrointestinal tract during the exposed phase of infection. Thus, even the population level viral

201 shedding function $f(t)$ used here may not accurately reflect the early viral shedding dynamics.

202 Furthermore, positive detection of SARS-CoV-2 virus was possible in only about 50% of samples

203 from infected individuals (8, 9), which suggests the possibility of gastrointestinal tract infection

204 being an inherent stochastic event. These important factors, among others, were not considered

205 in our study due to limited data but should be analyzed further to better understand and improve
206 the utility of WBE.

207

208

209 **SI References**

210

- 211 1. T. Phan, et al., A simple SEIR-V model to estimate COVID-19 prevalence and predict
212 SARS-CoV-2 transmission using wastewater-based surveillance data. *Sci. Total*
213 *Environ.* 857, 159326 (2023).
- 214 2. O. E. Hart, R. U. Halden, Computational analysis of SARS-CoV-2/COVID-19
215 surveillance by wastewater-based epidemiology locally and globally: Feasibility,
216 economy, opportunities and challenges. *Sci. Total Environ.* 730, 138875 (2020).
- 217 3. B. Killingley, et al., Safety, tolerability and viral kinetics during SARS-CoV-2 human
218 challenge in young adults. *Nature Med.* 28(5), 1031-1041 (2022).
- 219 4. R. Ke, et al., Daily longitudinal sampling of SARS-CoV-2 infection reveals substantial
220 heterogeneity in infectiousness. *Nat. Microbiol.* 7(5), 640-652 2022..
- 221 5. R. Ke, C. Zitzmann, D. D. Ho, R. M. Ribeiro, A. S. Perelson, In vivo kinetics of SARS-
222 CoV-2 infection and its relationship with a person's infectiousness. *Proc. Natl. Acad. Sci.*
223 *U.S.A.* 118(49), e2111477118 (2021).
- 224 6. F. Wu, et al., SARS-CoV-2 RNA concentrations in wastewater foreshadow dynamics
225 and clinical presentation of new COVID-19 cases. *Sci. Total Environ.* 805, 150121
226 (2022).
- 227 7. A. Xiao, et al., Metrics to relate COVID-19 wastewater data to clinical testing dynamics.
228 *Water Res.* 212, 118070 (2022).
- 229 8. S. Gupta, J. Parker, S. Smits, J. Underwood, S. Dolwani, Persistent viral shedding of
230 SARS-CoV-2 in faeces—a rapid review. *Colorectal Dis.* 22(6), 611-20 (2020).
- 231 9. A. Natarajan, et al., Gastrointestinal symptoms and fecal shedding of SARS-CoV-2 RNA
232 suggest prolonged gastrointestinal infection. *Med* 3(6), 371-387 (2022).